

Fine-grained Multiple Supervisory Network for Multi-modal Manipulation Detecting and Grounding

Xinquan Yu¹, Wei Lu^{1*}, Xiangyang Luo^{2*}

¹School of Computer Science and Engineering, Ministry of Education Key Laboratory of Information Technology, Guangdong Province Key Laboratory of Information Security Technology, Sun Yat-sen University, Guangzhou 510006, China

²State Key Laboratory of Mathematical Engineering and Advanced Computing, Zhengzhou 450002, China
yuxq28@mail2.sysu.edu.cn, luwei3@mail.sysu.edu.cn, luox_yie@sina.com

Abstract

The task of Detecting and Grounding Multi-Modal Media Manipulation (DGM⁴) is a branch of misinformation detection. Unlike traditional binary classification, it includes complex subtasks such as forgery content localization and forgery method classification. Consider that existing methods are often limited in performance due to neglecting the erroneous interference caused by unreliable unimodal data and failing to establish comprehensive forgery supervision for mining fine-grained tampering traces. In this paper, we present a Fine-grained Multiple Supervisory (FMS) network, which incorporates modality reliability supervision, unimodal internal supervision and cross-modal supervision to provide comprehensive guidance for DGM⁴ detection. For modality reliability supervision, we propose the Multimodal Decision Supervised Correction (MDSC) module. It leverages unimodal weak supervision to correct the multi-modal decision-making process. For unimodal internal supervision, we propose the Unimodal Forgery Mining Reinforcement (UFMR) module. It amplifies the disparity between real and fake information within unimodal modality from both feature-level and sample-level perspectives. For cross-modal supervision, we propose the Multimodal Forgery Alignment Reasoning (MFAR) module. It utilizes soft-attention interactions to achieve cross-modal feature perception from both consistency and inconsistency perspectives, where we also design the interaction constraints to ensure the interaction quality. Extensive experiments demonstrate the superior performance of our FMS compared to state-of-the-art methods.

Introduction

In the era of self-media, misinformation has proliferated due to its high popularity and substantial traffic (Lazer et al. 2018; Wu et al. 2019). Particularly with the iteration of generative models (Goodfellow et al. 2020; Ho, Jain, and Abbeel 2020), creating misinformation has become easier than ever. For instance, a simple command is sufficient to generate face images or text content with inconsistent attributes (Radford et al. 2019; Patashnik et al. 2021; Kang et al. 2023; Liu et al. 2024a), which seriously distorts event truths and disrupts public perception.

To address this, researchers have undertaken studies on detecting misinformation. Early methods primarily focused on unimodal data, such as fake text (Ma et al. 2015) and fake

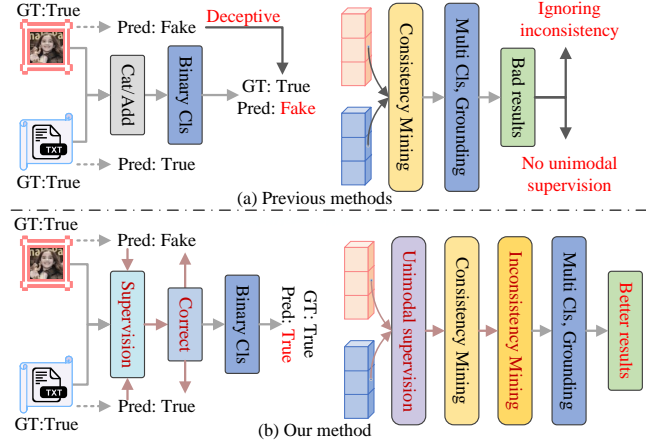


Figure 1: Comparison of the forgery supervision. (a) Previous methods combine features in a linear manner, which may be misleading due to unreliable modalities. And, previous methods focus on consistency mining. (b) Our method supervises and corrects for unreliable modalities, while enabling comprehensive supervision through unimodal supervision together with cross-modal consistency and inconsistency mining.

images (Gupta et al. 2013). With the advancement of the internet, multimodal data (Shu et al. 2020) has become the mainstream form of information transmission. This has led to the emergence of multimodal misinformation detection.

Early research on multimodal misinformation detection (Jin et al. 2017; Zhou et al. 2023; Ying et al. 2023) only supports binary classification of authenticity, largely due to the limitations of available datasets. With the proposal of the DGM⁴ dataset (Shao, Wu, and Liu 2023), research has shifted toward finer-grained detection (Liu et al. 2025), including forgery content localization and forgery method classification. It mainly includes: HAMMER (Shao, Wu, and Liu 2023) utilized a two-stage network to handle simple and complex subtasks separately. Building on this, HAMMER++ (Shao et al. 2024) devised a local viewpoint contrast loss to further align cross-modality features. Considering the inequality of cross-modal interactions, ViKI (Li et al. 2024) utilized the cross-modality prompt to adaptively aggregate

*Corresponding authors

unimodal embeddings, thereby leveraging complementary knowledge in cross-modality embedding. Since previous approaches primarily mined the manipulated traces from the RGB domain and overlooked the role of the frequency domain, UFAFormer (Liu et al. 2024b) utilized the discrete wavelet transform to enrich image representation for the first time. To mitigate performance degradation caused by modal competition, MSF (Wang et al. 2024) proposed the decoupled fine-grained classifiers to independently guide image and text features. In the state-of-the-art method ASAP (Zhang et al. 2025), the Large Language Model (LLM) was employed to enhance cross-modal alignment.

Although existing methods have yielded promising results, challenges still persist in the fine-grained understanding of forgery traces. As shown in Figure 1(a), this can be attributed to the following reasons, 1) Neglecting the erroneous interference from unreliable modality. Current methods treat the two unimodal features equally, typically employing concatenation or addition for binary classification. However, not all modality judgments are reliable. When an unreliable modality is present, utilizing such methods may lead to erroneous outcomes due to the disruptive influence of the unreliable unimodal feature. 2) Incomprehensive forgery supervision. Current methods primarily focus on supervising alignment and interaction of cross-modal information from the perspective of consistency, neglecting the role of inconsistent components within cross-modal information in forgery detection. Although the recent approach ASAP (Zhang et al. 2025) utilizes a tamper-guided cross-attention module to constrain interaction, it overlooks the consistency among cross-modal features. Furthermore, few existing methods impose constraints on the mining of forgery traces within individual modalities.

To this end, we propose the Fine-grained Multiple Supervisory Network (FMS), aimed at providing fine-grained constraints for DGM⁴ to guide the detection of subtle tampering traces. Specifically, as shown in Figure 1(b), to mitigate the erroneous interference from unreliable modalities, we design the Multimodal Decision Supervised Correction (MDSC) module. It first imposes weakly supervised constraints on each modality to assess its reliability, and then corrects the unreliable modality through contrastive learning. Next, to mine tampering traces within individual modalities, we design the Unimodal Forgery Mining Reinforcement (UFMR) module. It first amplifies the gap between real and fake features within a single image or text at the feature-level perspective, and then enhances the gap across multiple images or texts at the sample-level perspective. Finally, to provide comprehensive forgery supervision, we design the Multimodal Forgery Alignment Reasoning (MFAR) module. It first filters consistent and inconsistent regions guided by the similarity of global features. Subsequently, it utilizes a learnable mask matrix to mine the consistency and inconsistency of cross-modal information through soft-attention interactions, while utilizing interaction constraints to supervise the quality of these interactions. Our contributions are summarized as follows:

- We introduce FMS, a fine-grained multiple supervisory network for multi-modal manipulation detecting and

grounding, aiming to provide comprehensive supervision for fine-grained mining of tampering traces.

- We devise the MDSC module to mitigate erroneous interference from unreliable modality for the first time.
- We propose the UFMR and MFAR modules that provide fine-grained constraints from within and across modalities, respectively. Thereby providing comprehensive forgery supervision for the DGM⁴ task.

Methodology

Overview

The architecture of our FMS is depicted in Figure 2. Specifically, the multimodal content containing text and images is first fed into the encoder to obtain the initialized embeddings, which are later enhanced by cross-modal interaction. Here, the post-interaction image and text features are denoted as $V = [V_{cls}, V_{pat}]$ and $T = [T_{cls}, T_{tok}]$, respectively. Then, V_{cls} and T_{cls} are fed into the Multimodal Decision Supervised Correction (MDSC) module, in which the unimodal weak supervision is applied to improve the accuracy of binary classification. Next, V_{pat} and T_{tok} are fed into the Unimodal Forgery Mining Reinforcement (UFMR) module to amplify forgery traces, by calculating the feature-level loss for a single image (or text) and the sample-level loss for multiple images (or texts). Subsequently, V_{pat} and T_{tok} are fed into the Multimodal Forgery Alignment Reasoning (MFAR) module to align multimodal forgery traces, which is achieved by feeding them into consistency and inconsistency interactions, respectively. Finally, the outputs of MFAR are fed into fine-grained judgment module to perform multi-label classification, image and text grounding.

Multimodal Decision Supervised Correction

Binary classification is a subtask in DGM⁴, aimed at determining whether the given multimodal content is authentic. To achieve this, previous approaches (Zhao et al. 2024; Jin et al. 2024; Zhang et al. 2025; Li et al. 2025) treat both the image and text modality equally, directly concatenating the two features for multimodal decision-making. However, the accuracy of multimodal decision-making is jointly influenced by both modalities, and once one modality provides misleading information, an unreliable judgment may result.

Inspired by (Zou et al. 2023), we leverage the unimodal weak supervision to correct the multimodal decision-making process. Specifically, V_{cls} and T_{cls} are first fed into modality-specific classifiers to obtain unimodal predictions. Based on the ground truth, we can compute unimodal prediction loss denoted as \mathcal{L}_{uni}^v and \mathcal{L}_{uni}^t . For example, \mathcal{L}_{uni}^v is calculated by

$$\mathcal{L}_{uni}^v = \text{Mean}(\mathbf{H}(\text{MLP}(V_{cls})), y_{b-cls}^v) \quad (1)$$

where \mathbf{H} denotes the cross entropy function, y_{b-cls}^v denotes binary classification labels for image modality. Note that the unimodal true labels in DGM⁴ do not necessarily coincide with the binary labels because of the presence of unimodal forgeries. Following (Zou et al. 2023), we divide the features into Positive pairs \mathbb{P} , Semi-positive pairs \mathbb{S} and Negative pairs \mathbb{N} . For \mathbb{P} , we pull the two closer together, prompt-

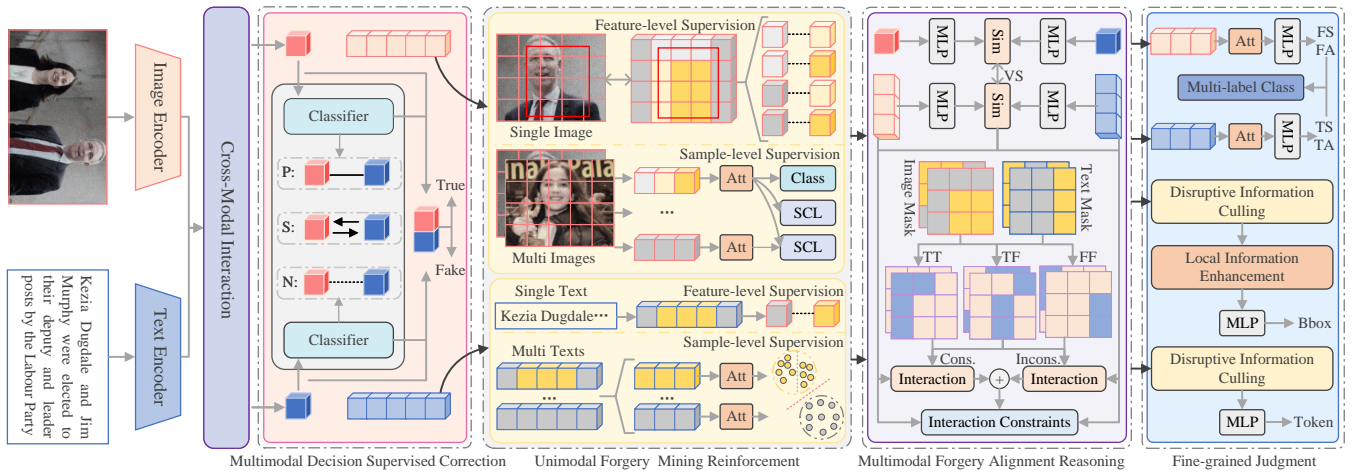


Figure 2: The overall architecture of proposed FMS. It consists of four components: (1) Multimodal Decision Supervised Correction: this module utilizes unimodal weakly supervised signals to supervise and correct multimodal decisions. (2) Unimodal Forgery Mining Reinforcement: this module amplifies unimodal forgery traces in terms of both feature-level and sample-level losses. (3) Multimodal Forgery Alignment Reasoning: this module ensures the alignment and inference of multimodal forgery traces based on consistency and inconsistency interactions. (4) Fine-grained Judgment: this module utilizes the attention aggregation and disruptive feature culling to achieve fine-grained decision-making.

ing them to become more similar. For \mathbb{S} , we pull the ineffective modality closer to the effective modality, prompting the ineffective modality to learn more useful information under weakly supervised signals. For \mathbb{N} , we push the two farther apart, making them more dissimilar. Thus, we can obtain the multimodal contrastive loss denoted as \mathcal{L}_{mmc} ,

$$\mathcal{L}_{mmc} = -\log \frac{\sum_{i \in \{\mathbb{P}, \mathbb{S}\}} \exp(\text{sim}(r_i^v, r_i^t) / \tau)}{\sum_{i \in \{\mathbb{P}, \mathbb{S}, \mathbb{N}\}} \exp(\text{sim}(r_i^v, r_i^t) / \tau)} \quad (2)$$

where r^v and r^t denote the unimodal representations of V_{cls} and T_{cls} after dimension reduction, respectively. $\text{sim}(\cdot)$ denotes the cosine similarity. $\tau = 0.07$ is utilized to control the difference degree. Finally, we concatenate V_{cls} and T_{cls} to perform binary classification and obtain the classification loss denoted as \mathcal{L}_{BIC} . Thus, the overall loss of MDSC can be expressed by

$$\mathcal{L}_{BIC}^* = \mathcal{L}_{BIC} + \alpha_1 * (\mathcal{L}_{uni}^v + \mathcal{L}_{uni}^t) + \alpha_2 * \mathcal{L}_{mmc} \quad (3)$$

where α_1 and α_2 are both trade-off hyperparameters to balance the losses.

Unimodal Forgery Mining Reinforcement

Multimodal detection is essentially an organic combination of multiple unimodal detection tasks, and its performance is closely linked to that of unimodal detection. To this end, UFMR is proposed to amplify the authenticity gap within unimodal features and mine the hidden forgery traces, thereby supporting accurate multimodal detection. It mainly consists two parts: feature-level supervision and sample-level supervision.

Feature-level Supervision. Feature-level supervision takes a single image (or text) as input, aiming to amplify the disparity between patch-to-patch (or token-to-token),

thereby enabling better segmentation of real and fake contents. In the case of images, we first divide the ViT-processed image patches into the following categories based on their overlap degree with the forged region,

$$\gamma_i = \begin{cases} 0 & \text{if } \mathcal{I}_i \in [0, 0.25\mathcal{P}] \\ 1 & \text{if } \mathcal{I}_i \in [0.25\mathcal{P}, 0.5\mathcal{P}] \\ 2 & \text{if } \mathcal{I}_i \in [0.5\mathcal{P}, 0.75\mathcal{P}] \\ 3 & \text{if } \mathcal{I}_i \in [0.75\mathcal{P}, \mathcal{P}] \end{cases} \quad (4)$$

where γ denotes the classified results of each patch. \mathcal{I} and \mathcal{P} denote the intersection area and patch area, respectively. Second, we arrange the above four categories to form four groups $\{\gamma \in \{0, 2\}\}$, $\{\gamma \in \{0, 3\}\}$, $\{\gamma \in \{1, 2\}\}$, $\{\gamma \in \{1, 3\}\}$. Then, we extract patch features from each group to amplify their differences,

$$\mathcal{L}_f^v = \text{Mean}(W_f^v \cdot \mathbf{H}(\sigma(\text{MLP}(V_{pat})_{\gamma})), (y_{pat})_{\gamma}) \quad (5)$$

where \mathcal{L}_f^v denotes the feature-level supervision for image modality, W_f^v denotes the corresponding adaptive weights, which are inversely proportional to the number of corresponding categories in the current group, thereby encouraging the method to assign higher weights to less numerous categories. σ denotes the Sigmoid function, $(y_{pat})_{\gamma}$ denotes fine-grained labels of image modality at position γ . For textual modality, we can similarly compute \mathcal{L}_f^t in a simpler manner. Finally, we can obtain the overall feature-level supervision loss,

$$\mathcal{L}_{FS} = \mathcal{L}_f^v + \mathcal{L}_f^t \quad (6)$$

Sample-level Supervision. Sample-level Supervision takes multiple images (or texts) as input, aiming to amplify the disparity between image-to-image (or text-to-text). In the case of images, we first filter out the real and fake

images based on the real labels y^v . Next, we execute a standard multi-head attention module (Vaswani et al. 2017) to fuse the features in different patch. Specifically, for real images, we have

$$\mathcal{G}_r^v = \text{MultiAtt}(g^v, V_{pat}^r, V_{pat}^r) \quad (7)$$

where g^v denotes the global image queries, which is a randomly initialized learnable embedding. V_{pat}^r denotes the local features in real images. For fake images, the situation is slightly different, as we only consider forged regions,

$$\mathcal{G}_f^v = \text{MultiAtt}(g^v, V_{pat}^f, V_{pat}^f, \mathcal{M}_{pat}^f) \quad (8)$$

where V_{pat}^f denotes the local features in fake images, \mathcal{M}_{pat}^f denotes the attention mask to ignore the real patches in the fake image. Then, \mathcal{G}_r^v and \mathcal{G}_f^v are fed into the Supervised Contrastive Learning (SCL) to enlarge the difference between real and fake images (Khosla et al. 2020),

$$\begin{aligned} \mathcal{L}_s^v = & -\text{Mean} \left(\frac{1}{|\mathcal{P}_i|} \sum_{j \in \mathcal{P}_i} \log \left(\frac{\exp(\wp_{ij})}{\sum_{k \neq i} \exp(\wp_{ik})} \right) \right) \\ & + \lambda \cdot \text{Mean} \left(\frac{1}{|\mathcal{N}_i|} \sum_{j \in \mathcal{N}_i} \wp_{ij} \right) \end{aligned} \quad (9)$$

where \mathcal{P}_i and \mathcal{N}_i denote positive and negative sample sets, respectively. $\wp = \text{sim}(\mathcal{G}_r^v, \mathcal{G}_f^v)/\tau$, $\lambda = 0.1$. For textual modality, we can also compute \mathcal{L}_s^t in the same way. Thus, the overall sample-level supervision loss is computed by

$$\mathcal{L}_{SS} = \mathcal{L}_s^v + \mathcal{L}_s^t \quad (10)$$

Since fake images are generated through two ways (face swap and face attributes manipulation) in DGM⁴ (Shao, Wu, and Liu 2023), the two leave different forged traces. For this reason, we further refine and supervise \mathcal{G}_f^v . We first perform

$$\mathcal{L}_{m^1}^v = \mathbf{H}(\sigma(\text{MLP}(\mathcal{G}_f^v)), y_m^v) \quad (11)$$

where $y_m^v = 1$ and $y_m^v = 0$ denote face swap and face attributes manipulation, respectively. Meanwhile, we still utilize the SCL to amplify the difference within \mathcal{G}_f^v , and obtain $\mathcal{L}_{m^2}^v$. Thus, we can compute $\mathcal{L}_m^v = \mathcal{L}_{m^1}^v + \mathcal{L}_{m^2}^v$ to assist the subsequent fine-grained face grounding task. For textual modality, the process is the same.

Multimodal Forgery Alignment Reasoning

Apart from enhancing unimodal forgery detection, as mentioned in the previous section, multimodal interaction and alignment are always regarded as a boon for multimodal forgery detection (Liu et al. 2024c; Yu et al. 2025). In this view, MFAR is proposed to align the detailed information of the two modalities, thereby supporting forgery detection. It mainly consists three layers: global supervision guidance, mask generation learning and soft interaction aggregation.

Global Supervision Guidance. This layer aims to construct consistency and inconsistency matrix while filtering out interfering information, through the supervised guidance of global features. Specifically, we first calculate the global similarity by

$$S_g = \text{sim}(\text{MLP}(V_{cls}), \text{MLP}(T_{cls})) \quad (12)$$

Second, we calculate the fine-grained similarity denoted as S_{p-t} between V_{pat} and T_{tok} in the same manner. Then, S_g and S_{p-t} are scaled between 0.5 and 1.5 to provide support for subsequent soft interaction. Third, we construct consistency matrix denoted as S_{max} utilizing the following constraints,

$$S_{max} = \begin{cases} S_{p-t} & \text{if } S_{p-t} > S_g \\ 0 & \text{otherwise} \end{cases} \quad (13)$$

while recording the number n_1 of selected features. If $n_1 < k$, we will supplement S_{max} by selecting $k - n_1$ additional distinct maximum values. Finally, we can also get cross-modality inconsistency matrix S_{min} in the same way.

Mask Generation Learning. This layer aims to construct learnable interaction masks to indicate the exact location of cross-modal consistent or inconsistent interactions. This can be divided into three cases: (1) For the regions where both the image and text are authentic, we apply consistency interaction. (2) For the regions with one authentic and one fake modality, we apply inconsistency interaction. (3) For the regions where both are fake, the two interactions mentioned above are applied.

Taking the first case as an example, we generate an initialized embeddings denoted as g_{tt} , to learn the masks when both modalities are authentic,

$$\mathcal{L}_{tt} = \text{Mean}(\mathbf{H}(\sigma(g_{tt})), y_{tt}) \quad (14)$$

where $y_{tt} = 1$ only when both modalities are authentic. Then, we can get g_{ff} and \mathcal{L}_{ff} in the same way. Thus, the consistent masks can be constructed based on the previously mentioned S_{max} ,

$$\chi_c = S_{max} \cdot (g_{tt} + \alpha_3 \cdot g_{ff}) \quad (15)$$

where $\alpha_3 = 0.5$ is utilized to control the weight of regions that both modalities are fake.

In the same way, the inconsistent masks is computed by

$$\chi_{ic} = S_{min} \cdot (g_{tf} + \alpha_3 \cdot g_{ff}) \quad (16)$$

where $g_{tf} = 1 - g_{tt} - g_{ff}$.

Soft Interaction Reasoning. This module aims to perform fine-grained cross-modal interactions from both consistent and inconsistent perspectives. In the case of consistency interactions for image modality, we have

$$\bar{V}_{pat} = V_{pat} + \text{softmax} \left(\frac{V_{pat} \cdot (T_{tok})^T}{\sqrt{d}} \right) \cdot \chi_c \cdot T_{tok} \quad (17)$$

Note that, unlike the hard-mask strategy in traditional attention mechanisms, our strategy not only filters out irrelevant information, but also adaptively controls the attention weights of the selected features, through χ_c . Second, we can

obtain \hat{V}_{pat} by utilizing χ_{ic} in the same way. Thus, the post-interaction image features denoted as \tilde{V}_{pat} can be obtained by

$$\tilde{V}_{pat} = \bar{V}_{pat} + \hat{V}_{pat} \quad (18)$$

Third, we further design interaction constraints, to ensure that the binary classification after interaction is accurate, and the detection performance is improved, compared to without interaction. This process is modeled as

$$\mathcal{L}_{ic}^v = \mathcal{L}_{ai}^v + \mathcal{L}_{ni}^v + \eta \cdot \Phi(\mathcal{L}_{ai}^v - \mathcal{L}_{ni}^v) \quad (19)$$

where \mathcal{L}_{ic}^v denotes the interaction constraints loss. η is a hyperparameter to control the punishment intensity. $\Phi(\cdot)$ denotes the ReLU activation function. \mathcal{L}_{ai}^v and \mathcal{L}_{ni}^v represent the detection loss after interaction and without interaction, respectively. Both of them have a similar calculation process. For example, \mathcal{L}_{ai}^v is computed by

$$\mathcal{L}_{ai}^v = \text{Mean} (W_{ai}^v \cdot \mathbf{H}(\sigma(\text{MLP}(\tilde{V}_{pat}))), y_{pat}) \quad (20)$$

For textual modality, we can compute \tilde{T}_{tok} and \mathcal{L}_{ic}^t in the same way. Thus, the overall cross-modal interaction loss is

$$\mathcal{L}_{CI} = \mathcal{L}_{tt} + \mathcal{L}_{ff} + \mathcal{L}_{ic}^v + \mathcal{L}_{ic}^t \quad (21)$$

Fine-grained Judgment

This module aims to utilize the features extracted above to achieve fine-grained decision-making, including multi-classification, image grounding and text grounding.

Multi Classification Task. Considering that the multi-classification task is an extension of the binary classification task, we utilize the features from binary classification to guide the multi-classification task. Taking image multi classification as an example, we have

$$V_c = V_{cls} + \text{MultiAtt}(V_{cls}, \tilde{V}_{pat}, \tilde{V}_{pat}) \quad (22)$$

Then, V^c is used to predict face fine-grained manipulation type including FS and FA, thus we can compute image fine-grained classification loss \mathcal{L}_{m-cls}^v following (Wang et al. 2024). For textual modality, we can also get T^c and \mathcal{L}_{m-cls}^t in the same manner. Thus, the overall multi-classification loss is

$$\mathcal{L}_{MLC}^* = \mathcal{L}_{mlc}^v + \mathcal{L}_{mlc}^t + \mathcal{L}_m^v + \mathcal{L}_m^t \quad (23)$$

where \mathcal{L}_m^v and \mathcal{L}_m^t are defined in the above section to achieve better supervision.

Grounding Tasks. For grounding tasks, we first propose a disruptive information culling layer to reduce the interference from cross-modal information. In the case of image grounding, we execute

$$V_g = \begin{cases} V_{pat} & \text{if } y_{b-cls}^v == 1 \ \& \ y_{b-cls}^t == 0 \\ \tilde{V}_{pat} & \text{otherwise} \end{cases} \quad (24)$$

This means that we utilize V_{pat} instead of \tilde{V}_{pat} for image localization only when the image is fake and the text is true, to avoid interference, and vice versa. Second, we utilize a

randomly initialized learnable embedding to learn global information with the supervision of V_{cls} ,

$$\mathcal{G}_g^v = \text{MultiAtt}(g_g^v, \text{Cat}(V_{cls}, V_g), \text{Cat}(V_{cls}, V_g)) \quad (25)$$

Then, \mathcal{G}_g^v is feed into the specific classifiers to achieve image grounding. Finally, for textual modality, we can obtain T_g and \mathcal{G}_g^t in the same way by using Eq. (24) and Eq. (25), respectively, so as to predict fake text content.

Full Objectives. Here we elaborate on all supervisions included in the proposed method. Specifically, there are two aspects of supervision involved, one is designed to improve detection performance, and the other is the original supervision from DGM⁴ (Shao, Wu, and Liu 2023). For the former, we combine all the losses involved,

$$\mathcal{L}_{our} = \mathcal{L}_{FS} + \mathcal{L}_{SS} + \mathcal{L}_{CI} \quad (26)$$

For the latter, we utilize the same supervision function as outlined in (Wang et al. 2024). Note that we enrich two original supervisions in Eq. (3) and Eq. (23) for binary-classification (\mathcal{L}_{BLC}^*) and multi-classification (\mathcal{L}_{MLC}^*) tasks, respectively. By optimizing both, we achieve multi-modal manipulation detection and grounding.

Experiments

Datasets and Metrics

All experiments in this paper are conducted on the DGM⁴ dataset (Shao, Wu, and Liu 2023), which contains four types of manipulation including Face Swap (FS), Face Attribute (FA), Text Swap (TS), and Text Attribute (TA). In more detail, it has 230,000 image-text pairs comprising 77,426 genuine pairs and 152,574 manipulated pairs. Among the manipulated pairs, there has 123,133 fake images (54% FS and 46% FA), 62,134 fake texts (70% TS and 30% TA) and 32,693 mixed-manipulation pairs that comprises 21% of all manipulated pairs.

For model evaluation, we adopt the same metrics as the previous approaches (Shao et al. 2024; Zhang et al. 2025). Specifically, ACC, AUC and EER are applied to evaluate the binary classification task. MAP, CF1 and OF1 are applied to evaluate the fine-grained multi-classification task. IoUmean, IoU50 and IoU75 are applied to evaluate the image grounding task. Precision, Recall, and F1-score are applied to evaluate the text grounding task.

Implementation Details

All experiments in this paper are conducted on 8 A100 GPUs. Specifically, for fairness, we first resize the images to 256×256 and pad the text to a length of 50. Subsequently, following previous studies (Wang et al. 2024; Li et al. 2025), we use ViT-B/16 (Dosovitskiy et al. 2020) and RoBERTa (Liu et al. 2019) to extract image and text features, respectively, with the pretraining weights loaded from METER (Dou et al. 2022), so as to obtain V and T . Additionally, all attention blocks mentioned in the paper consist of 4 layers, with a dropout rate of 0. During the training phase, we use AdamW as the optimizer with the weight decay of 0.02 and learning rate of 1×10^{-5} . Finally, we train for 50 epochs with a batch size of 32, and select the weights from the last epoch for testing.

	Method	Reference	Binary Cls			Multi-label Cls			Image Grounding			Text Grounding		
			AUC	EER↓	ACC	mAP	CF1	OF1	IoUmean	IoU50	IoU75	Precision	Recall	F1
Entire Dataset	CLIP	ICML21	83.22	24.61	76.40	66.00	59.52	62.31	49.51	50.03	38.79	58.12	22.11	32.03
	ViLT	ICML21	85.16	22.88	78.38	72.37	66.14	66.00	59.32	65.18	48.10	66.48	49.88	57.00
	HAMMER	CVPR23	93.19	14.10	86.39	86.22	79.37	80.37	76.45	83.75	76.06	75.01	68.02	71.35
	HAMMER++	TPAMI24	93.33	14.06	86.66	86.41	79.73	80.71	76.46	83.77	76.03	73.05	72.14	72.59
	UFAFormer	IJCV24	93.81	13.60	86.80	87.85	80.31	81.48	78.33	85.39	79.20	73.35	70.73	72.02
	MSF	ICASSP24	95.11	11.36	88.75	91.42	83.60	84.38	80.83	88.35	80.39	76.51	70.61	73.44
	IDseq	AAAI25	94.55	11.40	88.94	90.01	83.00	84.90	83.33	89.39	86.10	75.96	71.23	73.52
	ASAP	CVPR25	94.38	12.73	87.71	88.53	81.72	82.89	77.35	84.75	76.54	79.38	73.86	76.52
	FMS (Ours)	-	96.46	9.65	90.54	93.43	86.80	87.68	84.82	91.00	88.03	79.43	71.66	75.34

Table 1: Comparison with state-of-the-art multi-modal methods on the entire DGM⁴. The best results are bold.

	Method	Reference	Binary Cls			Image Grounding		
			AUC	EER↓	ACC	IoUmean	IoU50	IoU75
Image Sub.	TS (Luo et al. 2021)	CVPR21	91.80	17.11	82.89	72.85	79.12	74.06
	MAT (Zhao et al. 2021)	CVPR21	91.31	17.65	82.36	72.88	78.98	74.70
	HAMMER (Shao, Wu, and Liu 2023)	CVPR23	94.40	13.18	86.80	75.69	82.93	75.65
	HAMMER++ (Shao et al. 2024)	TPAMI24	94.69	13.04	86.82	75.96	83.32	75.80
	ViKI (Li et al. 2024)	IF24	91.85	15.92	84.90	75.93	82.16	74.57
	UFAFormer (Liu et al. 2024b)	IJCV24	94.88	12.35	87.16	77.28	85.46	78.29
	FMS (Ours)	-	97.31	8.21	91.67	83.45	90.60	87.17

Table 2: Comparison between our FMS and unimodal methods on the image subset of DGM⁴. The best results are bold.

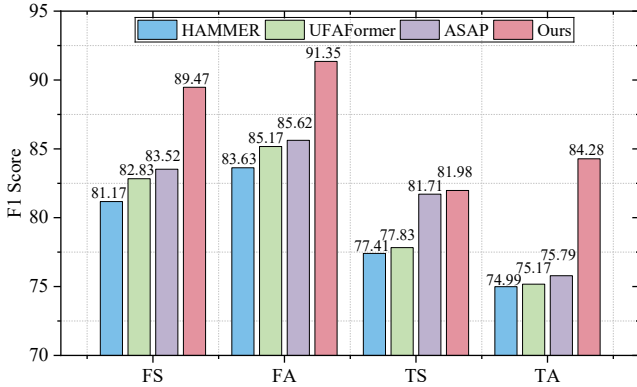


Figure 3: Comparison about fine-grained classification of forged methods.

Comparison with the State-of-the-Art Methods

Comparison with Multi-modal Methods. Table 1 shows the comparison results between our FMS and eight state-of-the-art methods on the entire DGM⁴ dataset.

It can be observed that our FMS outperforms all the comparative methods mentioned above and achieves the highest performance. Specifically, for the binary classification task, our FMS achieves 96.46% AUC, improving by 1.35%–13.24% over the comparison method, while improving 2.08% on the latest proposed ASAP (Zhang et al. 2025). For the multi classification task, our FMS achieves 93.43% mAP, improving by 2.01%–27.43% over the comparison method, while improving 4.90% on ASAP. What’s more, for

image grounding task, our FMS attains 84.82% IoUmean, 91.00% IoU50 and 88.03% IoU75. Compared to ASAP, we gains +7.47%, +6.25% and +11.49% on IoUmean, IoU50 and IoU75, respectively. For text grounding task, our FMS attains 75.34% F1, gaining +1.82% over IDseq (Liu et al. 2025). However, our approach is slightly inferior to ASAP because it enriches textual information with LLM.

Besides, we conduct comparative experiments on the fine-grained classification of forgery methods. As shown in Figure 3, our method consistently outperforms HAMMER, UFAFormer and ASAP. For example, for FS, our method gains +8.30%, +6.64% and +5.95% over HAMMER, UFAFormer and ASAP, respectively. For TA, our method gains +9.29%, +9.11% and +8.49% over HAMMER, UFAFormer and ASAP, respectively. This reflects the effectiveness of fine-grained multiple supervision of FMS.

Comparison with Unimodal Methods. Similar to previous methods (Shao et al. 2024; Liu et al. 2024b), we conduct comparisons with unimodal methods on the image and text subsets, respectively. Table 2 shows the comparison results for the image subset, where the image is forged. It can be noticed that our FMS attains the best scores with 97.31% AUC, 91.67% ACC, 83.45% IoUmean, 91.00% IoU50, 87.17% IoU75, which significantly outperforms the other methods. Compared with MAT (Zhao et al. 2021), our FMS gains +6.00% AUC, +9.31% ACC, +10.57% IoUmean and +12.47% IoU75. We consider that this is because MAT only mined tamper traces from the image viewpoint and neglected the text contribution for multimodal detection. In contrast, our approach achieves performance improvement by utilizing multimodal learning.

	Method	Reference	Binary Cls			Text Grounding		
			AUC	EER↓	ACC	Precision	Recall	F1
Text Sub.	BERT (Devlin et al. 2019)	NAACL19	80.82	28.02	68.98	41.39	63.85	50.23
	LUKE (Yamada et al. 2020)	EMNLP20	81.39	27.88	76.18	50.52	37.93	43.33
	HAMMER (Shao, Wu, and Liu 2023)	CVPR23	93.44	13.83	87.39	70.90	73.30	72.08
	HAMMER++ (Shao et al. 2024)	TPAMI24	93.49	13.58	87.81	72.70	72.57	72.64
	ViKI (Li et al. 2024)	IF24	92.31	15.27	85.35	78.46	65.09	71.15
	UFAFormer (Liu et al. 2024b)	IJCV24	94.11	12.61	84.71	81.13	70.73	75.58
	FMS (Ours)	-	96.35	9.67	89.88	84.81	71.66	77.68

Table 3: Comparison between our FMS and unimodal methods on the text subset of DGM⁴. The best results are bold.

Method	Binary Cls			Multi-label Cls			Image Grounding			Text Grounding		
	AUC	EER↓	ACC	mAP	CF1	OF1	IoUmean	IoU50	IoU75	PR.	Recall	F1
w/o MDSC	95.91	9.92	90.23	92.94	86.53	87.26	84.00	90.26	86.96	78.00	71.36	74.53
w/o UFMR	96.07	9.79	90.27	93.22	86.56	87.25	81.45	89.37	80.44	78.99	71.51	75.07
w/o MFAR	95.45	9.87	90.31	93.13	86.74	87.50	84.17	90.48	87.13	78.55	71.85	75.05
Full	96.46	9.65	90.54	93.43	86.80	87.68	84.82	91.00	88.03	79.43	71.66	75.34

Table 4: Ablation study of FMS with different components. PR. represents precision. The best results are bold.



Figure 4: Visualization of detection and grounding results. Here, red box and text indicate the prediction of manipulated faces and words, while green box and text represent the corresponding ground truth.

Table 3 shows the comparison results for the text subset, where our method is also the best. Especially in the text grounding task, our method gains +27.45% F1 and +34.35% F1 on BERT and LUKE, respectively. Compared with UFAFormer, our FMS also improves 2.24% AUC, 5.17% ACC and 2.10% F1.

Ablation Study

To verify the necessity of the proposed components, we removed MDSC, UFMR, and MFAR, respectively. The results are shown in Table 4, where the performance of the full method is the best. Specifically, when removing MDSC, the classification performance decreases significantly, where mAP decreases by 0.49%. When removing UFMR or MFAR, the grounding performance is also im-

paired. This sufficiently demonstrates that each of the mentioned components is meaningful for DMG⁴.

In addition, we devise a baseline, which directly utilizes the features after cross-modal interactions for detection and localization. The visualized comparison results are shown in Figure 4. It can be seen that our method better mines the fine-grained tampering traces.

Conclusion

In this paper, we propose a framework named FMS to provide comprehensive supervision for tampering trace mining. We first introduce MDSC to assess modality reliability and correct the erroneous interference of unreliable modality. Second, we develop UFMR to supervise the disparity between real and fake information within unimodal

data, thereby enhancing the forgery detection capability of unimodal features. Finally, we present MFAR to align cross-modal features from both consistency and inconsistency perspectives, thereby facilitating effective interaction between cross-modal information. Extensive experiments demonstrate that FMS significantly outperforms comparable methods, especially on the image grounding task, where we gain more than 8% on average over the latest method.

References

- Devlin, J.; Chang, M.-W.; Lee, K.; and Toutanova, K. 2019. Bert: Pre-training of deep bidirectional transformers for language understanding. In *Proceedings of the North American Chapter of the Association for Computational Linguistics: Human Language Technologies*, 4171–4186.
- Dosovitskiy, A.; Beyer, L.; Kolesnikov, A.; Weissenborn, D.; Zhai, X.; Unterthiner, T.; Dehghani, M.; Minderer, M.; Heigold, G.; Gelly, S.; et al. 2020. An image is worth 16x16 words: Transformers for image recognition at scale. *arXiv preprint arXiv:2010.11929*.
- Dou, Z.-Y.; Xu, Y.; Gan, Z.; Wang, J.; Wang, S.; Wang, L.; Zhu, C.; Zhang, P.; Yuan, L.; Peng, N.; et al. 2022. An empirical study of training end-to-end vision-and-language transformers. In *Proceedings of the IEEE/CVF Conference on Computer Vision and Pattern Recognition*, 18166–18176.
- Goodfellow, I.; Pouget-Abadie, J.; Mirza, M.; Xu, B.; Warde-Farley, D.; Ozair, S.; Courville, A.; and Bengio, Y. 2020. Generative adversarial networks. *Communications of the ACM*, 63(11): 139–144.
- Gupta, A.; Lamba, H.; Kumaraguru, P.; and Joshi, A. 2013. Faking sandy: Characterizing and identifying fake images on twitter during hurricane sandy. In *Proceedings of the 22nd International Conference on World Wide Web*, 729–736.
- Ho, J.; Jain, A.; and Abbeel, P. 2020. Denoising diffusion probabilistic models. *Advances in Neural Information Processing Systems*, 33: 6840–6851.
- Jin, R.; Fu, R.; Wen, Z.; Zhang, S.; Liu, Y.; and Tao, J. 2024. Fake news detection and manipulation reasoning via large vision-language models. *arXiv preprint arXiv:2407.02042*.
- Jin, Z.; Cao, J.; Guo, H.; Zhang, Y.; and Luo, J. 2017. Multimodal fusion with recurrent neural networks for rumor detection on microblogs. In *Proceedings of the 25th ACM International Conference on Multimedia*, 795–816.
- Kang, M.; Zhu, J.-Y.; Zhang, R.; Park, J.; Shechtman, E.; Paris, S.; and Park, T. 2023. Scaling up gans for text-to-image synthesis. In *Proceedings of the IEEE/CVF Conference on Computer Vision and Pattern Recognition*, 10124–10134.
- Khosla, P.; Teterwak, P.; Wang, C.; Sarna, A.; Tian, Y.; Isola, P.; Maschinot, A.; Liu, C.; and Krishnan, D. 2020. Supervised contrastive learning. *Advances in Neural Information Processing Systems*, 33: 18661–18673.
- Lazer, D. M.; Baum, M. A.; Benkler, Y.; Berinsky, A. J.; Greenhill, K. M.; Menczer, F.; Metzger, M. J.; Nyhan, B.; Pennycook, G.; Rothschild, D.; et al. 2018. The science of fake news. *Science*, 359(6380): 1094–1096.
- Li, Q.; Gao, M.; Zhang, G.; Zhai, W.; Chen, J.; and Jeon, G. 2024. Towards multimodal disinformation detection by vision-language knowledge interaction. *Information Fusion*, 102: 102037.
- Li, Y.; Yang, Y.; Tan, Z.; Liu, H.; Chen, W.; Zhou, X.; and Lei, Z. 2025. Unleashing the Potential of Consistency Learning for Detecting and Grounding Multi-Modal Media Manipulation. In *Proceedings of the IEEE/CVF Conference on Computer Vision and Pattern Recognition*, 9242–9252.
- Liu, A.; Feng, B.; Xue, B.; Wang, B.; Wu, B.; Lu, C.; Zhao, C.; Deng, C.; Zhang, C.; Ruan, C.; et al. 2024a. Deepseek-v3 technical report. *arXiv preprint arXiv:2412.19437*.
- Liu, H.; Tan, Z.; Chen, Q.; Wei, Y.; Zhao, Y.; and Wang, J. 2024b. Unified frequency-assisted transformer framework for detecting and grounding multi-modal manipulation. *International Journal of Computer Vision*, 1–18.
- Liu, R.; Xie, T.; Li, J.; Yu, L.; and Xie, H. 2025. IDseq: Decoupled and Sequentially Detecting and Grounding Multi-Modal Media Manipulation. In *Proceedings of the AAAI Conference on Artificial Intelligence*, volume 39, 496–504.
- Liu, X.; Yu, Y.; Li, X.; and Zhao, Y. 2024c. MCL: Multimodal contrastive learning for deepfake detection. *IEEE Transactions on Circuits and Systems for Video Technology*, 34(4): 2803–2813.
- Liu, Y.; Ott, M.; Goyal, N.; Du, J.; Joshi, M.; Chen, D.; Levy, O.; Lewis, M.; Zettlemoyer, L.; and Stoyanov, V. 2019. Roberta: A robustly optimized bert pretraining approach. *arXiv preprint arXiv:1907.11692*.
- Luo, Y.; Zhang, Y.; Yan, J.; and Liu, W. 2021. Generalizing face forgery detection with high-frequency features. In *Proceedings of the IEEE/CVF Conference on Computer Vision and Pattern Recognition*, 16317–16326.
- Ma, J.; Gao, W.; Wei, Z.; Lu, Y.; and Wong, K.-F. 2015. Detect rumors using time series of social context information on microblogging websites. In *Proceedings of the 24th ACM International Conference on Information and Knowledge Management*, 1751–1754.
- Patashnik, O.; Wu, Z.; Shechtman, E.; Cohen-Or, D.; and Lischinski, D. 2021. Styleclip: Text-driven manipulation of stylegan imagery. In *Proceedings of the IEEE/CVF International Conference on Computer Vision*, 2085–2094.
- Radford, A.; Wu, J.; Child, R.; Luan, D.; Amodei, D.; Sutskever, I.; et al. 2019. Language models are unsupervised multitask learners. *OpenAI blog*, 1(8): 9.
- Shao, R.; Wu, T.; and Liu, Z. 2023. Detecting and grounding multi-modal media manipulation. In *Proceedings of the IEEE/CVF Conference on Computer Vision and Pattern Recognition*, 6904–6913.
- Shao, R.; Wu, T.; Wu, J.; Nie, L.; and Liu, Z. 2024. Detecting and grounding multi-modal media manipulation and beyond. *IEEE Transactions on Pattern Analysis and Machine Intelligence*.
- Shu, K.; Mahudeswaran, D.; Wang, S.; Lee, D.; and Liu, H. 2020. FakeNewsNet: A data repository with news content, social context, and spatiotemporal information for studying fake news on social media. *Big Data*, 8(3): 171–188.

- Vaswani, A.; Shazeer, N.; Parmar, N.; Uszkoreit, J.; Jones, L.; Gomez, A. N.; Kaiser, Ł.; and Polosukhin, I. 2017. Attention is all you need. *Advances in Neural Information Processing Systems*, 30.
- Wang, J.; Liu, B.; Miao, C.; Zhao, Z.; Zhuang, W.; Chu, Q.; and Yu, N. 2024. Exploiting modality-specific features for multi-modal manipulation detection and grounding. In *Proceedings of the IEEE International Conference on Acoustics, Speech and Signal Processing*, 4935–4939.
- Wu, L.; Morstatter, F.; Carley, K. M.; and Liu, H. 2019. Misinformation in social media: Definition, manipulation, and detection. *ACM SIGKDD Explorations Newsletter*, 21(2): 80–90.
- Yamada, I.; Asai, A.; Shindo, H.; Takeda, H.; and Matsumoto, Y. 2020. LUKE: Deep contextualized entity representations with entity-aware self-attention. *arXiv preprint arXiv:2010.01057*.
- Ying, Q.; Hu, X.; Zhou, Y.; Qian, Z.; Zeng, D.; and Ge, S. 2023. Bootstrapping multi-view representations for fake news detection. In *Proceedings of the AAAI Conference on Artificial Intelligence*, volume 37, 5384–5392.
- Yu, X.; Sheng, Z.; Lu, W.; Luo, X.; and Zhou, J. 2025. RaCMC: Residual-aware compensation network with multi-granularity constraints for fake news detection. In *Proceedings of the AAAI Conference on Artificial Intelligence*, volume 39, 986–994.
- Zhang, Z.; Wang, Y.; Cheng, L.; Zhong, Z.; Guo, D.; and Wang, M. 2025. ASAP: Advancing semantic alignment promotes multi-modal manipulation detecting and grounding. In *Proceedings of the IEEE/CVF Conference on Computer Vision and Pattern Recognition*, 4005–4014.
- Zhao, H.; Zhou, W.; Chen, D.; Wei, T.; Zhang, W.; and Yu, N. 2021. Multi-attentional deepfake detection. In *Proceedings of the IEEE/CVF Conference on Computer Vision and Pattern Recognition*, 2185–2194.
- Zhao, W.; Lu, Y.; Jiao, G.; and Yang, Y. 2024. Concentrated Reasoning and Unified Reconstruction for Multi-Modal Media Manipulation. In *Proceedings of the IEEE International Conference on Acoustics, Speech and Signal Processing*, 8190–8194.
- Zhou, Y.; Yang, Y.; Ying, Q.; Qian, Z.; and Zhang, X. 2023. Multimodal fake news detection via clip-guided learning. In *Proceedings of the IEEE International Conference on Multimedia and Expo*, 2825–2830.
- Zou, H.; Shen, M.; Chen, C.; Hu, Y.; Rajan, D.; and Chng, E. S. 2023. UniS-MMC: Multimodal classification via unimodality-supervised multimodal contrastive learning. *arXiv preprint arXiv:2305.09299*.